Trans Indian Inst Met (2020) 73(5):1227–1237
https://doi.org/10.1007/s12666-020-01971-3

ORIGINAL ARTICLE

Effect of Reversible Cyclic Plastic Deformation and Thermal Treatment on the Microstructure and Mechanical Properties of SS304L Steel

Ranveer Singh[1] · S. Sharma[2] · S. K. Vajpai[1]

Received: 23 February 2020 / Accepted: 6 April 2020 / Published online: 27 April 2020

Abstract In the present study, the effect of heat treatment and reversible cyclic plastic deformation (RCPD) on microstructure and mechanical properties of stainless steel 304L (SS304L) has been examined. The RCPD demonstrated a significant reduction in the grain size as well as formation of deformation-induced twins, without any observable phase transformation in the SS304L specimens. An isothermal annealing of as-received specimens at 950 °C (1223 K) for varying annealing durations exhibited the formation of recrystallized equiaxed austenitic microstructure. It was also observed that the grain size and the twin width increased simultaneously with annealing time, wherein the grain size increased linearly, whereas the increment in the twin width was parabolic in nature. The density of deformation twins decreased with increasing annealing time, which was attributed to the variation in the stacking fault energy (SFE) with temperature and duration of annealing treatment. The average hardness values decreased with increasing annealing time, and this trend was correlated with the increasing grain sizes and, simultaneously, decreasing amount of twin density.

Keywords Severe plastic deformation · Mechanical properties · Stainless steel · Twinning · Stacking fault energy

✉ S. Sharma
swati.meta@mnit.ac.in

[1] Department of Metallurgical and Materials Engineering, National Institute of Technology, Jamshedpur, India

[2] Department of Metallurgical and Materials Engineering, Malaviya National Institute of Technology, Jaipur, India

1 Introduction

Steel is one of the most widely used materials in a variety of structural applications. In particular, SS304L austenitic stainless steel is one of the most widely used steels offering optimum combination of strength, ductility, excellent corrosion resistance and good weldability [1]. With such remarkable properties, these steels find vast use in transportation, nuclear, chemical, bio-structural and aerospace industries [2]. However, there always remains a requirement of further improvement in the mechanical properties of steels due to ever increasing demand of high-performance components, particularly due to miniaturization of components, and expanding the regime of applications of these steels towards new areas. Such requirements have pushed the demand to produce steels with varied combinations of strength and ductility, while maintaining its excellent chemical and other properties intact.

It is well known that the mechanical properties are altered either by changing the chemical composition, i.e. alloying additions, or by altering microstructure through various thermal, mechanical or thermo-mechanical treatments. In case of austenitic steels, microstructural modifications, such as variation in grain size and size distribution, are one of the prominent strategies to achieve desired mechanical properties. In particular, grain refinement via different mechanical and thermo-mechanical methods is the most readily adopted strengthening mechanism to improve the strength and toughness of austenitic steels. In addition to grain refinement, the presence of twins, deformation as well as annealing twins, also leads to significant strengthening in the materials. Hence, a combination of twins and grain size can result in a significant impact on the mechanical properties [3].

In case of face-centred cubic (fcc) crystals, annealing twins are formed during recrystallization and grain growth, which is attributed to migrating grain boundaries [4]. It has also been suggested that there is a considerable impact of pre-straining in the material which causes the annealing twins to form easily during annealing. The first brief discussion on the nature and formation of annealing twins was presented by Carpenter and Tamura [5] which was followed by several other works discussing the dependence of grain size and twins [6]. Gertsman et al. [7] have investigated and shown the interdependency of annealing twins on the texture which has a direct impact on the mechanical properties of the polycrystalline materials. It was also concluded that the evolving grain size distribution is a result of the multiple annealing twins.

The stacking fault energy (SFE) is a major factor which decides the deformation mechanism and mechanical property of a material, i.e. SFE decides whether the deformation would take place with martensitic transformation, by twinning, or by gliding of the dislocations, which in turn indicates the mechanical strengthening. SFE lower than the 18 mJ m^{-2} favours the martensitic transformation [8], whereas in the range of the 18–45 mJ m^{-2} twins are generated easily [9, 10]. Having a high SFE causes the dislocation to have a smooth glide. It is well known that austenitic steels have low SFE, and both deformation and annealing twins are easily formed in SS304L grade steels. As a result, SS304 grade steels show common features of thin twins and twin bundles in the microstructure which effectively contribute to work hardening and thermal stability [11–14]. Thus, an increase in the twin density shows higher strength and hardness in the material, which holds true for both deformation as well as annealed twins [15, 16].

The twin generation depends upon the grain size and orientation of the grains in the polycrystalline materials as also reported by Lee and Urrutia [17, 18]. Twin density variation with the size of grain and SFE has also been reported at many occasions [19, 20]. Both the deformation and annealing twins are identical crystallographically, with stacking faults along the consecutive {111} planes in the case of FCC crystals [21]. Cold working on the SS 304L increases the strength with a moderate decrease in the ductility of the material, wherein the dislocation–dislocation interaction, twin–twin interaction and the dislocation twin interaction cause increase in the strength (strain hardening) of materials [22]. Another factor which affects the annealing twin formation is the annealing time. Initially, the deformation twin density decreases and above a certain annealing time, annealing twin starts forming easily and its density increases thereafter. This is attributed to the low stacking fault energy leading to the formation of annealing twins. It was proposed by Mathewson [23] that the formation of annealing twins happens by lateral growth of thin deformation twins at the time of heat treatment of FCC crystals, whereas Murr et al. showed the interdependency of twin thickness with the pre-deformation rate [24].

Another important role in the enhancement of mechanical properties like hardness, strength and ductility is attributed to the thermal stability of the deformation twins. However, the understanding of thermal stability of the deformation twins is quite limited and needs a systematic investigation on the generation and impact of deformation twins on the properties of materials. From the literature, there is no clear evidence for the temperature dependence of thermal stability of deformation twins in case of SS304L. However, it has time and again been reported that the thermal stability has a strong dependence on the processing of materials based on which the temperature for thermal stability varies with the type of deformation process. In the case of Fe–Mn–C steel, deformation twins have been found to be stable up to 550 °C for 60-min heat treatment [25], whereas the deformation twins generated by pre-straining in TWIP steel with high manganese at ambient temperature have been reported to be stable up to 625 °C (recrystallization temperature) [26]. In the present work the effect of annealing time and temperature on thermal stability of the twins have also been studied to a certain extent.

During the production of any metallic component, materials undergo several types of mechanical, thermal and thermo-mechanical processing. As a result, a variety of microstructural features appear in the finished products which, in turn, affect the mechanical properties of the components. Therefore, with all the view points, the present study was aimed to investigate the effect of RCPD and thermal treatments on the microstructural parameters, such as grain size, twin density and twin width, on the SS304L steel sheets and their correlation with the mechanical properties. It was also attempted to establish the correlation of the prior processing history of the SS304L sheets with the microstructural evolution during subsequent mechanical and thermal processing. Furthermore, the efforts were also made to investigate the stability of the twins at high temperature for different annealing time. The results of RCPD and thermal treatments on the microstructural evolution in a SS304L grade stainless steel sheet and their effect on the resulting mechanical properties have been presented and discussed. Furthermore, results related to the correlation of the prior processing history of SS304L on the microstructural evolution during subsequent RCPD at ambient temperature and thermal treatments have also been presented and discussed.

2 Experimental Procedure

The steel used in the present study is a commercial austenitic stainless steel 304L (SS304L) having an average composition as shown in Table 1. The as-received sample was in the form of sheet of 1 mm thickness. These as-received samples had a prior history of being pre-strained during the sheet formation. Rectangular strips of dimensions 30 mm × 50 mm were cut in order to perform further investigations.

In the first set of experiments, a few as-received samples were subjected to (RCPD) technique by using a standard cupping test arrangement, as shown in Fig. 1. The as-received SS304L specimens were pressed with a load of 20 KN against an indenter to give a deformation to the sheet at room temperature. The RCPD processing included 5 steps, viz. (i) pressing the sample with the punch having round tip (Fig. 1b), (ii) flattening the sample by the hydraulic press (Fig. 1c), (iii) then rotating the sample by 180° along the axis of the plane of the sheet (Fig. 1d), then (iv)repeating the pressing by punch (Fig. 1e) and (v) flattening again using hydraulic press (Fig. 1f). The number of cycles was restricted to 6 (introducing von Mises plastic strain of 0.22 in each deformation step at the centre of the specimen, as estimated through numerical simulation of the deformation process using ANSYS software), to ensure that the amount of RCPD was limited to avoid the cracking as surface cracks were found to appear after 7–8 cycles at the same level of applied strain. This deformation process ensured almost negligible dimensional changes while straining the specimens. In the second set of experiments, the as-received specimens were subjected to isothermal annealing at 950 °C (1223 K) in a muffle furnace for different time durations, i.e. 30 min, 90 min, 180 min and 360 min, followed by water quenching at room temperature.

Optical microscope (OM) was used to investigate the variation in the microstructure due to varying annealing time of the specimens and effect of the RCPD. For higher magnifications, the same specimens were subsequently examined under the scanning electron microscopy (SEM). For microstructural characterization of the deformed specimens, samples were taken from the most strained region of the specimen in order to obtain true representation of the deformation that has taken place. Specimens for metallography were conventionally prepared by initially paper polishing with the help of SiC abrasive papers of grit size 400–2000. This was followed by cloth polishing with the help of fine alumina suspension having particle size of 1 and 0.05 μm which was the final polishing in this case in order to obtain a mirror-like surface finish. Then, the etching was done with the help of Carpenter stainless steel etchant (8.5 g ferric chloride, 2.4 gm cupric chloride, 122 ml ethanol, 122 ml hydrochloric acid, 6 ml nitric acid) in order to reveal the microstructure of the specimens. The mechanical properties of the specimens were evaluated through hardness measurements of the specimens via Vickers microhardness tester. Nominal load of 100 g for a time period of 5 s was used to produce the indent on the surface. These tests were performed on the surface of each specimen having varying annealing time. For each annealing condition, five numbers of samples were tested in order to obtain an average hardness value. In the case of deformed specimen, indentations were made at the centre, i.e. most strained region of the specimen, to estimate the average hardness. The constituent phases in specimens with different processing conditions were identified by X-ray diffraction (XRD) using phase diffractometer. The diffractometer was operated at 30 kV and 10 mA using a Cu target, wavelength of 1.5406 Å with a scan rate of 1° per minute and scanning range of 2θ was from 40° to 100°. For measuring the grain size from the microstructure, linear intercept method as well as the measurement of size of the individual grains was used. In case of individual grain size measurements, 150 numbers of grains were considered for each condition, which gave the final average grains size. The twin density calculated was the average number of twin's interaction per unit length along the grains [27], whereas twin width was evaluated by linear analysis method proposed by Smith et al. [28]. The calculation of twin width is the space between two adjacent twin boundaries. The twin width for each sample was calculated by taking an average of about 300–400 twins, wherein approximately 150 grains were taken into consideration. The results are presented and discussed in the following section.

Table 1 Chemical composition of as-received SS 304L

Elements	C	Si	Mn	Cr	Ni	P	M	Fe
Composition (wt%)	0.039	0.334	1.03	18.60	8.92	0.043	0.138	Balance

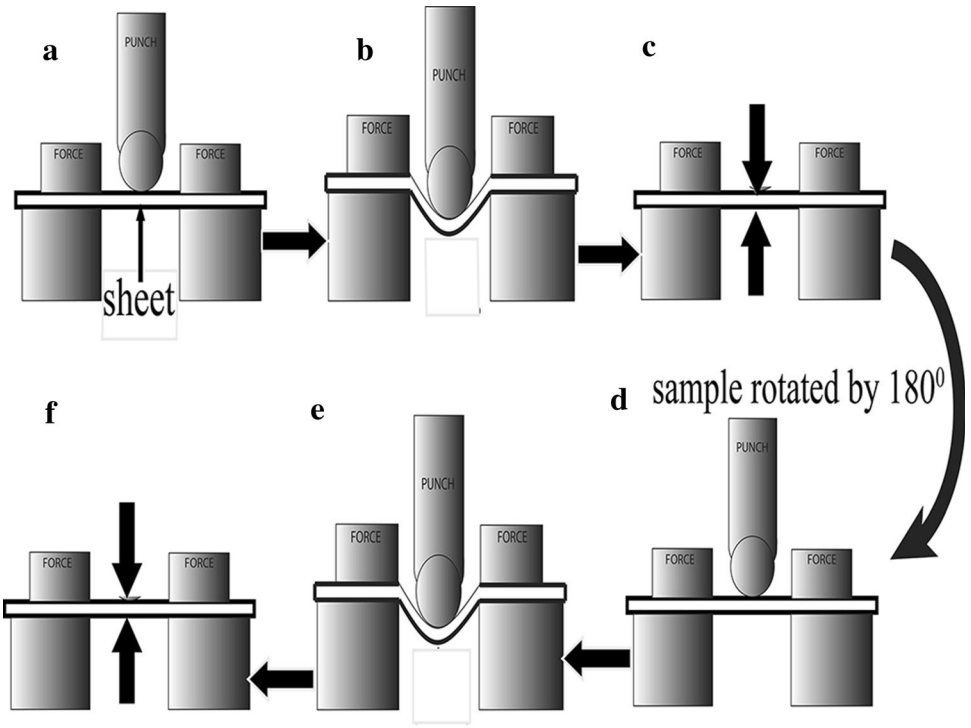

Fig. 1 Sequence of steps used in one cycle of RCPD process on SS304L plate

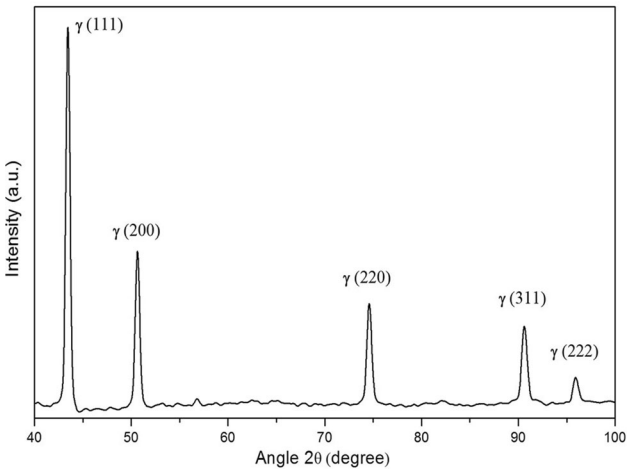

Fig. 2 X-ray diffraction pattern of as-received SS 304L specimen

3 Results and Discussion

3.1 Microstructure of As- received specimen

Figure 2 shows the XRD patterns of the as-received specimen. Five major peaks have been indexed and identified as peaks corresponding to (111), (200), (220), (311) and (222) planes of face-centred cubic (fcc) phase. The diffraction pattern clearly reveals the presence of only single-phase face-centred cubic (fcc) crystal structure, i.e. austenite. Figure 3a, b shows the microstructures of the as-received specimen at low and high magnifications, respectively. The microstructure clearly shows the presence of elongated grains of an average grain size 70 ± 5 μm, having lamella of fine as well as wide twins, which appears to be dependent on the size of the grains as the finer grains appear to consist of relatively finer twins as compared to coarse grains. The presence of elongated grains clearly indicates that the pre-straining is an effect of rolling on the as-received sheet specimen, leading to the orientation of the grains in the direction of rolling. Figure 3c shows the SEM image illustrating the internal microstructure of the as-received specimens. We can still observe some elongated grains and a lot of deformation twins within grains as marked by the arrows. These observations clearly indicate the dependency of width of deformation twins on the size of the grains.

It is believed that the requirement of stress for the formation of deformation twins is mainly controlled by the amount of stacking fault energy (SFE) of the materials. The SFE can be determined by the major compositional constituents present in the austenitic stainless steel. Its calculations given by Schramm et al. [29] have been used in the present study to calculate the same.

$$\mathrm{SFE} = -53 + 6.2(\text{pct Ni}) + 0.7(\text{pct Cr}) + 3.2(\text{pct Mn}) + 9.3(\text{pct Mo})\left(\mathrm{mJ/m^2}\right).$$

A value of 21 $\mathrm{mJ/m^2}$ for the present material has been obtained using this equation which is in agreement with the data presented by Murr [24] suggesting that the given material lies within the range of materials that prefer to go

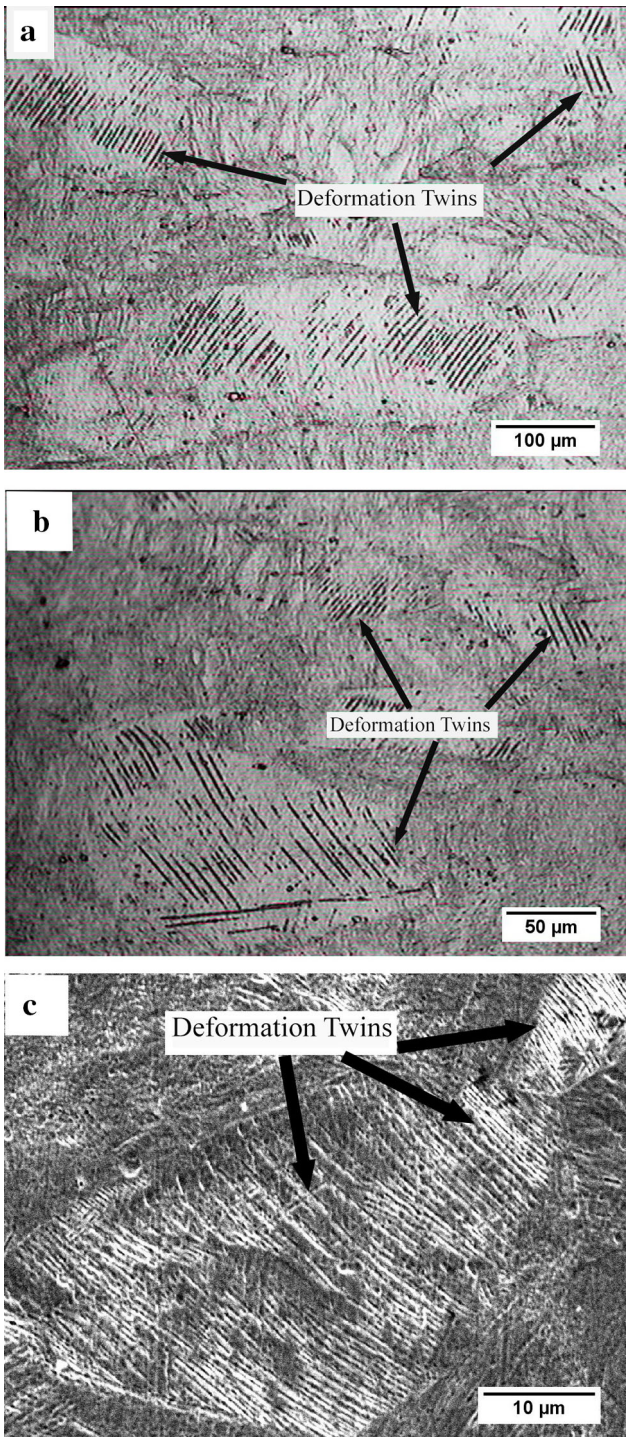

Fig. 3 Optical micrographs of as-received specimens: **a** low magnification, **b** high magnification and **c** SEM micrographs of as-received specimen

through the twin deformation mode rather than the slip mode. Therefore, due to lower stacking fault energy (SFE) of SS 304L, deformation in the form of twins is quite easy in comparison with other modes.

Besides having a significant effect on the grain size, the extent of deformation also has effect on the twins, especially in the case of deformation twins, i.e. the increase in deformation causes dislocation density to increase. When a critical dislocation density is achieved, deformation twins are formed in the material [30]. There are several reports available on the formation of deformation twins in various FCC structural materials [31–38]. Hence, in the as-received SS304L sheet, the presence of deformed grain structure together with fine-size twins suggests that deformation twins are formed during pre-rolling of the sheet due to lower stacking fault energy (SFE) of SS304 which results in strain accumulation via twinning mode rather than any other mode of deformation.

3.2 Effect of Reversible Cyclic Plastic Deformation (RCPD)

Figure 4 shows the XRD patterns of the RCPD specimens of the SS304L. The XRD pattern of the as-received specimen is also provided in the same figure for comparison. It can be noticed that the overall XRD pattern after RCPD remains more or less similar to that of the as-received specimen. The similarity of XRD patterns of as-received and RCPD specimens, i.e. the absence of appearance of any new or extra peak, is an evidence of the absence of any deformation-induced phase transformation leading to appearance of any new phase in the material after the deformation, i.e. the FCC crystal structure of the parent material remains untransformed due to RCPD. In general, it has been observed that the SS304 grade leads to the formation of deformation-induced martensite when subjected to large plastic deformation at room temperature. However, it becomes very difficult to ascertain such transformation through XRD analysis when the extent of

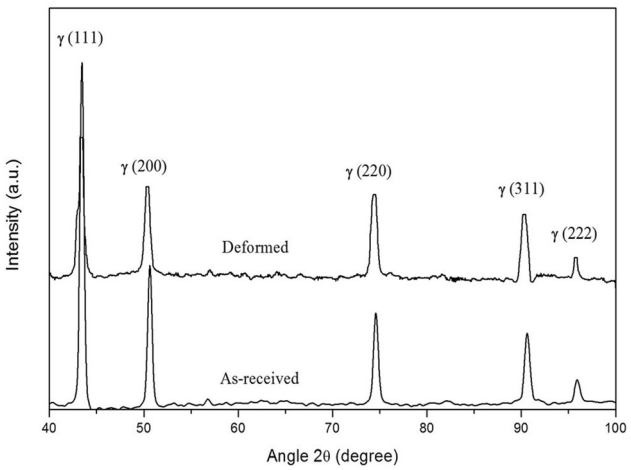

Fig. 4 X-ray diffraction patterns of as-received and RCPD specimens

plastic deformation and phase transformation is not very significant due to the fact that there are common peaks associated with the austenite and martensite phases. Therefore, formation of some amount of strain-induced martensite cannot be ruled out in the present case.

It is also worth mentioning that relative width of XRD peaks of the deformed specimens is significantly larger, especially at low angles, than that of the corresponding peaks of as-received specimens. The comparison of values of full-width-half-maxima (FWHM) of various XRD peaks of as-received and deformed specimen is shown in Table 2. It can also be observed that the relative intensity of the XRD peaks of the deformed specimen is significantly lower as compared to those of the corresponding peaks of as-received samples. The relative intensity reduction and broadening of the XRD peaks are generally associated with the plastic deformation-induced lattice straining and grain refinement.

RCPD-processed specimens show the microstructure of the deformed specimens at the centre of the specimen (i.e. most strain region of the specimen) shown in Fig. 5 at different magnifications wherein the presence of only single phase in the deformed specimen can be clearly observed. These results are in accordance with the XRD pattern of RCPD specimen. However, it is interesting to note that the RCPD specimens exhibit the presence of high density of deformation twins within the grains. Moreover, the grain refining in the RCPD is evident with grain size reduction from 70 ± 5 μm in the as-received samples to 48 ± 3 μm after RCPD shown in Fig. 5a, b. These observations indicate that the RCPD results in slight increment in the deformation-induced twins and a significant reduction in the grain size as compared to that of the as-received samples, and Fig. 5c shows the SEM micrograph of the same RCPD specimens which also shows the presence of smaller size of grains and multiple deformation twins, of the order of nano-meter thickness, within the fine-sized grains as marked by the arrows. These observations clearly indicate the dependency of width of deformation twins on the size of the grains.

3.3 Effect of Isothermal Heat Treatment on the As-received SS304L

The as-received specimens were heat-treated in a muffle furnace at 950 °C (1223 K) for holding time of 90 min, 180 min and 360 min. Figure 6 shows the XRD patterns of the isothermally heat-treated specimens, together with that of as-received specimens. A comparison of the XRD patterns shows no significant characteristic changes in the overall pattern, relative peak positions and peak width, with increasing holding time. However, XRD peak intensity appears to be increasing with holding time. Therefore, these results clearly indicate that the increasing holding time during heat treatment at 950 °C (1223 K) does not lead to any phase transformation. However, the possibility of partial recrystallization or a slight grain growth cannot be ruled out.

Figure 7a–d shows the optical micrographs of the as-received specimens after annealing at 950 °C(1223 K) with varying holding time of 30 min, 90 min, 180 min and 360 min. The optical micrographs of the annealed specimen reveal recrystallized equiaxed grains with twinned structure for all the specimens. The average grain sizes of the samples annealed for 30, 90, 180 and 360 min are found to be 85 ± 7 μm, 98 ± 8 μm, 122 ± 10 μm and 166 ± 10 μm, respectively. These observations demonstrate an obvious grain growth with increase in the holding duration. However, it can also be observed from the micrographs that the deformation twins are predominant over annealing twins for both 30-min- and 90-min-annealed specimens (Fig. 7a, b). This observation is based on the fact that, generally, annealing twins are relatively wider as compared to deformation twins [39]. Interestingly, it can also be observed that there is a presence of higher density of deformation twins as compared to annealing twins. A similar trend has also been reported by Tewary et al. [39] wherein the presence of both deformation and annealing twins, simultaneously, in the same microstructure and the predominance of deformation twins has been reported. However, deformation twins appear to be thermally stable at 950 °C up to 90 min of holding time as there is no observable coarsening of these twins with increasing annealing time (Fig. 7a, b). In case of specimens annealed

Table 2 FWHM values of parent specimens and deformed specimens

Sr. no.	2 Theta value of XRD peaks	Plane of peaks	FWHM value of parent specimens	FWHM value of deform specimens
1	43.36	(111)	0.5051	0.6910
2	50.38	(200)	0.5383	0.6851
3	74.40	(220)	0.6012	0.7262
4	90.323	(311)	0.6764	0.7061

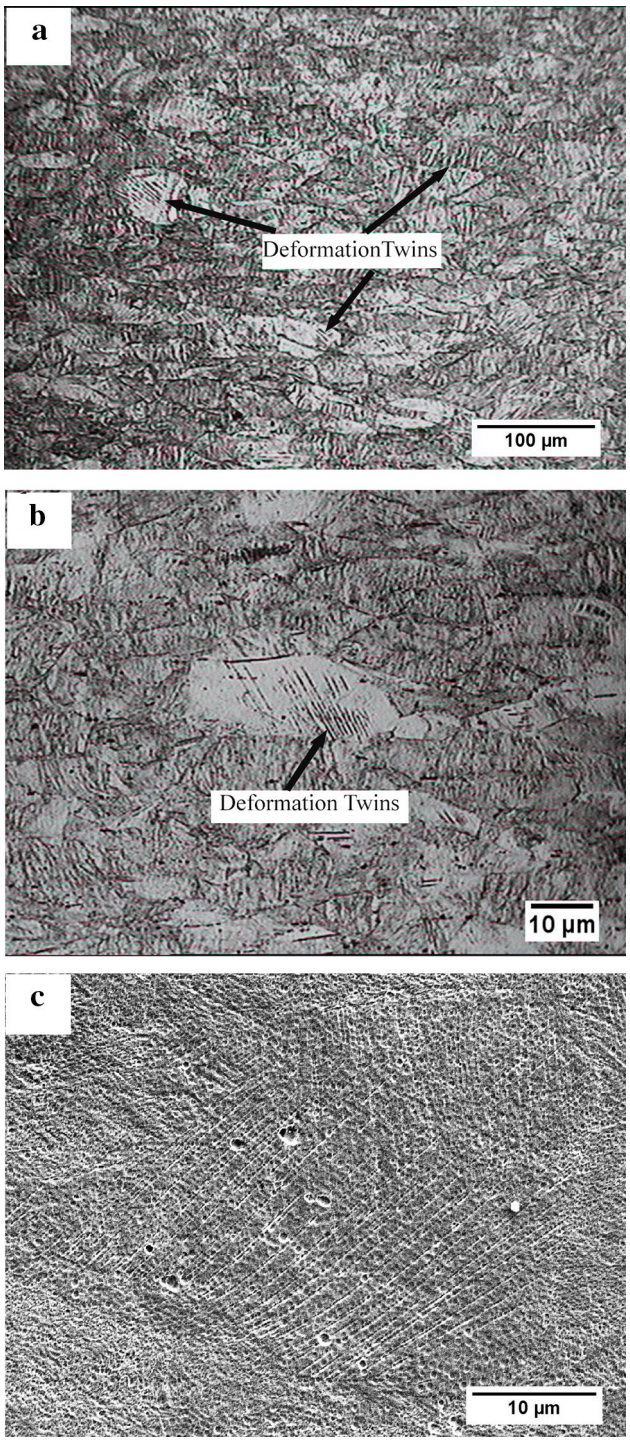

Fig. 5 Optical micrograph of RCPD specimens: **a** low magnification, **b** high magnification and **c** SEM micrograph

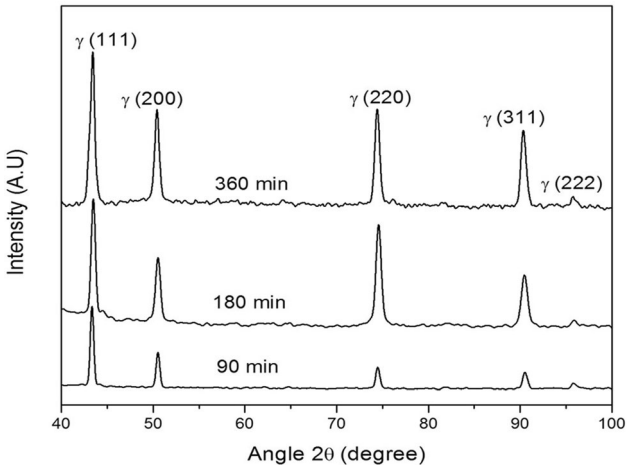

Fig. 6 X-ray diffraction patterns of heat-treated specimens at 950 °C (1223 K) for a varying holding duration of 90 min, 180 min and 360 min

for 180 min (Fig. 7c), it can be observed that the presence of deformation twins is insignificant in comparison with that of annealing twins. These observations clearly indicate that the annealing time of 180 min leads to significant grains growth as well as replacement of deformation twins with the annealing twins. Further, as shown in Fig. 7d, the microstructure of the specimen annealed at 360 min exhibits the presence of only annealing twins. However, the twin density appears to be higher than that of the specimens annealed up to 180 min.

As observed above, the deformation gradually decreases from twins of 30-min-annealed specimen to 90-min-annealed specimen and gets completely exhausted for the specimens annealed for 180 min and 360 min. The reduction in deformation twins can be related to the occurrence of de-twinning as the holding time increases. The occurrence of de-twinning is quite easy for the thin deformation twins as the driving force in twin–twin interaction is attributed to the variation of the excess energy of the two twin boundaries [40]. Therefore, the above results clearly demonstrate that the deformation twins decreases with increasing annealing time and, progressively, vanishes for the annealing duration greater than 90 min. This trend may be attributed to the relatively higher thermal stability of annealing twins than that of deformation twins.

Figure 8 shows the variation of the twin width as a function of increasing annealing time. The variation of grain size as a function of annealing time is also plotted on the same figure to understand the correlation between twin width and grain size. It can be noticed that grain size increases almost linearly with increasing annealing time. The range of the average grain size varies from 85 ± 7 µm for the 30-min-annealed specimens to 166 µm for specimens annealed for up to 360 min of annealing time. From Fig. 8, it can be clearly indicated that there is a continuous growth in twin width with the annealing duration. It is interesting to note that grain size and twin width increase simultaneously with annealing time. However, it can also be noted that the grain size increases linearly with annealing time, whereas the increment in the twin width is

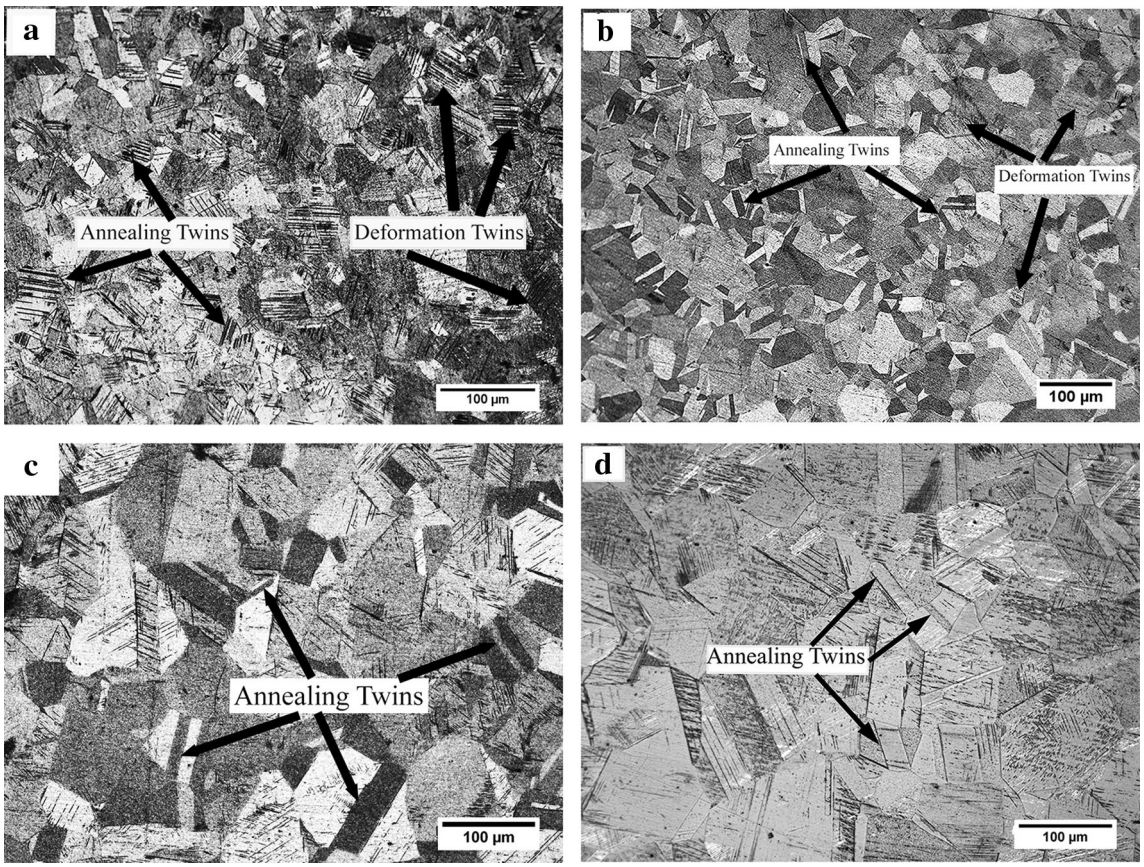

Fig. 7 Optical micrograph of heat-treated specimens at 950 °C (1223 K) for varying holding duration **a** 30 min, **b** 90 min, **c** 180 min and **d** 360 min

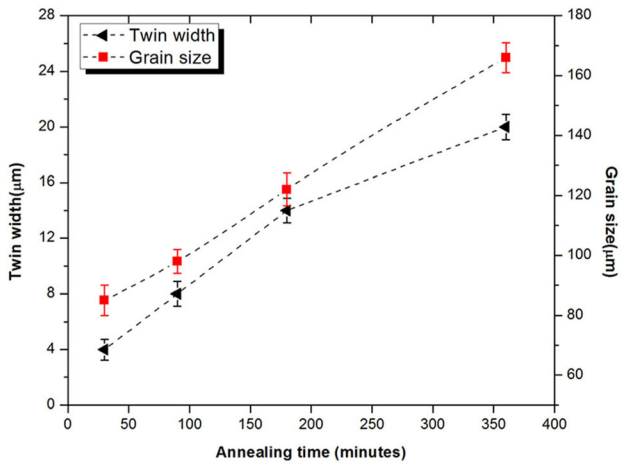

Fig. 8 Variation in twin width and grain size with the increasing annealing duration at isothermal temperature of 950 °C (1223 K)

parabolic in nature. Moreover, it can also be noticed that the rate of growth of grains and the rate of thickening of twins are almost similar up to 180 min of annealing, i.e. almost linear, and the perceivable deviation in the growth rate of twins starts appearing after 180 min of annealing time. These observations suggest that the grain size is not the only factor affecting the twin coarsening during annealing, and the other factors also seem to play an important role in limiting the coarsening of twins. In previous reports, it has been indicated that the grain growth is accompanied by coarsening of twins due to the formation and migration of incoherent twin boundaries (ITB) [40, 41]. Moreover, it has also been reported that the migration of ITBs promotes lateral migration of coherent twin boundaries (CTBs), leading to an increase in the twin width. Since the relatively thinner twins are expected to consist of more coherent boundaries as compared to the thicker twins, the thinner twins can be expected to coarsen faster than their thicker counterparts. As a result, the rate of thickening will be relatively faster in the early stages and it is expected to slow down with increasing annealing time as the thickening of twins occurs [40, 41].

3.4 Mechanical Properties

Figure 9 shows the plot of Vickers hardness for different conditions of specimens for average hardness values obtained from microindentation using 100 g load. Each hardness value reported here is an average of

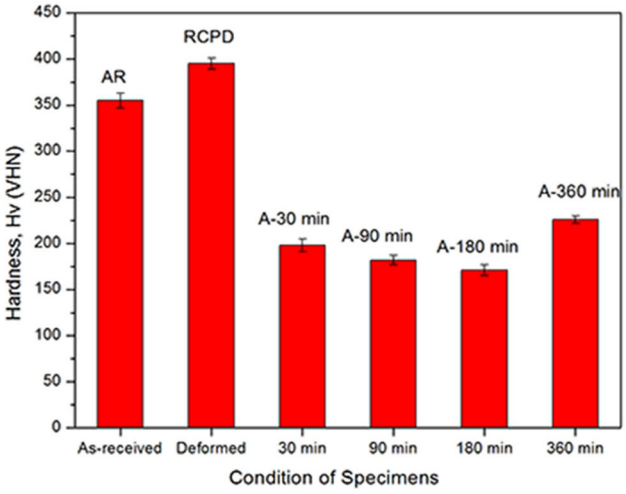

Fig. 9 Hardness values of as-received, RCPD and heat-treated specimens of SS304L

approximately 15 indents for each condition. These average values along with their standard deviation are plotted in Fig. 9. It can be observed that the average hardness value increases from 358 ± 12 to 395 ± 8 Hv for the as-received specimen and deformed specimen, respectively. Such an increment can be attributed to the observable grain refining, as observed from the micrograph of the deform specimen and also slight increment in the deformation twin density as shown in Fig. 10. Similar trend has also been observed in the several studies [42–44], wherein the role of decrease in ductility after RCPD due to strain hardening is also one of the key factors contributing towards this observed trend.

In the case of as-received specimens that have been annealed at 950 °C (1223 K) for different holding durations, it is interesting to note that average microhardness

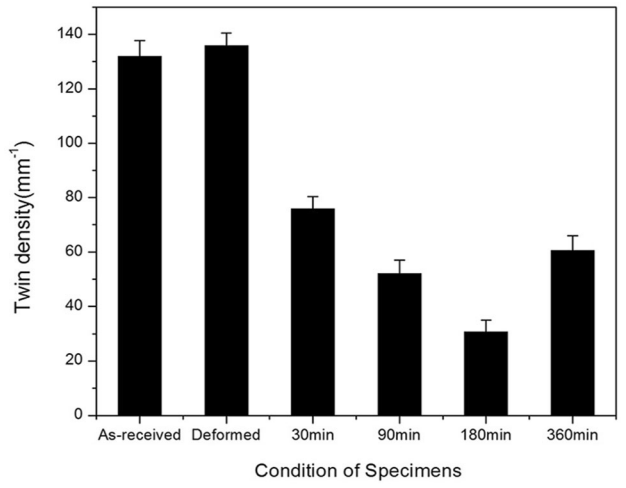

Fig. 10 Twin density values for as-received, RCPD and heat-treated specimens of SS304L

value decreases significantly after isothermal annealing for holding time of 30 min. The average hardness value is obtained to be 198 ± 10 Hv. It can also be observed that the average hardness further decreases from 181 ± 7 to 170 ± 5 Hv as a result of increasing the annealing duration from 90 to 180 min. Such a continuously decreasing average hardness values can be correlated with the increasing ductility due to recrystallization with continuously increasing grain sizes and, simultaneously, decreasing amount of twin density. The average hardness of the 360-min-annealed specimens again increases significantly, achieving the average value of 226 ± 10 Hv. Generally, the hardness is expected to decrease with increasing annealing holding duration due to annealing of stored microstructural defects and grain growth. However, it is interesting to note that the hardness value of the specimen with a holding time of 360 min is significantly higher than that of specimen annealed for holding time of 30 min, 90 min and 180 min. This anomaly can be attributed to the fact that there is a significant increase in the twin density for samples annealed for a duration of 360 min, leading to observed increase in the hardness of these samples. A similar significant increment in the average hardness value due to increase in twin density has been reported by Somekawa et al. [15].

3.5 Thermal Stability of Deformation Twins

Figure 10 shows the average twin density of as-received, RCPD, annealed specimens. It can be observed that there is only a slight increment in the twin density of as-received specimens and the deformed specimen with the values of average twin density 132 mm^{-1} and 136 mm^{-1}, respectively. These results suggest that the pre-rolling in the as-received specimen has resulted in a high twin density, which appears to be almost the saturation value for the present material considering the fact that the subsequent deformation results only in a slight increment in the twin density. On the other hand, the annealing of the as-received specimens demonstrate that there is a sudden decrease in the twin density of 30-min-annealed specimen (76 mm^{-1}) followed by a decreasing trend of twin density as the holding time further increases. For 90 min and 180 min annealing time, the twin density have been found to be 52 mm^{-1} and 30 mm^{-1}, respectively. The decrease in the twin density from 90-min-annealed specimen to 180-min-annealed sample is attributed to the disappearance of deformation twins, as discussed earlier. However, it is interesting to note that a further increase in the annealing time up to 360 min exhibits a sudden increment in the twin density (60 mm^{-1}) as compared to that of the 180-min-annealed specimens (30 mm^{-1}), which can be attributed to the formation of large number of annealing twins due to the

prolonged annealing duration. The annealing out of the deformation twins can be related to the variation in the SFE with temperature and duration of annealing treatment. It appears that an annealing at 950 °C (1223 K) and increasing the holding time beyond 90 min affect the SFE to such an extent that the deformation twins almost disappear due to the sliding of the dislocations, which becomes feasible as the SFE exceeds the threshold limit for the dislocation to glide. As a result, a gradual decrease in the case of deformation twin density is observed as the holding time increases from 30 min specimen to 360 min for SS304L specimens.

In case of 316L SS, it has been reported that the deformation twins are stable up to 60 min of annealing time at 800 °C, wherein the samples are processed through equal channel angular extrusion (ECAE) [14]. Furthermore, the tensile specimens with 30% elongation results in the formation of nano-twins, which are found to be thermally stable up to 60 min at 900 °C [45]. On the contrary, it has also been reported that the thermal stability of the deformation twins is lost after 60-min heat treatment at 600 °C when a specimen of 316L SS is cold-rolled up to thickness reduction of 37% [46]. However, it must be emphasized that, in the case of SS304L in the present study, the deformation twins are thermally stable up to 950 °C. These observations suggest that the thermal stability of deformation twins of pre-rolled SS304L is considerably higher as compared to those of cold-rolled SS316L deformed up to approximately 37% thickness reduction.

4 Conclusions

The following conclusions can be drawn from the present work:

1. The as-received sheets exhibited the presence of elongated grains, of average size 70 ± 5 μm, with lamella of fine and coarse deformation twins, wherein the finer grains appeared to consist of relatively finer twins as compared to larger grains. The formation of deformation twins during pre-rolling of the sheet was attributed to the lower SFE of SS304L which resulted in strain accumulation via twinning mode rather than any other mode of deformation.
2. The RCPD resulted in a significant reduction in the grain size as well as small increment in deformation-induced twins, as compared to that of the as-received samples. Also, the reversible cyclic plastic deformation (RCPD) did not induce any observable phase transformation in the SS304L specimens. The average hardness value increased RCPD which was attributed to the observable grain refining and the slight increment in the deformation twin density.
3. An isothermal annealing of as-received specimens at 950 °C for varying holding time led to the formation of recrystallized equiaxed microstructure, consisting of austenitic phase, wherein the grain size increased almost linearly with increasing holding time.
4. It was demonstrated that the deformation twins decreased with increasing annealing time and, progressively, vanished for the annealing duration greater than 90 min. The reduction in the deformation twins was attributed to the occurrence of de-twinning as the holding time increased.
5. It was observed that the grain size and twin width increased simultaneously with annealing time. However, the grain size increased linearly with annealing time, whereas the increment in the twin width was parabolic in nature.
6. The average hardness values decreased, continuously, with increasing annealing time. The decreasing average hardness values were correlated with the increasing ductility due to recrystallization with continuously increasing grain sizes and, simultaneously, decreasing amount of twin density.
7. The density of deformation twins decreased with increasing annealing time. The annealing out of the deformation twins was related to the variation in the SFE with temperature and duration of annealing treatment.

References

1. Shen Y F, Li X X, Sun X, Wang YD, and Zuo L, *Mater Sci Eng A* **552** (2012) 514.
2. Ye C, Telang A, Gill A S, Suslov S, Idell Y, Zweiacker K, Wiezorek J M K, Zhou Z, Qian D, Mannava S R, and Vasudevan V K, *Mater Sci Eng A* **613** (2014) 274.
3. Mahajan S, *Scripta Mater* **68** (2013) 95.
4. Gleiter H, *Acta Metall* **17** (1969) **1421**.
5. Carpenter H C H, and Tamura S, *Proc R Soc A Math Phys Eng Sci* **113** (1926) 161. https://doi.org/10.1098/rspa.1926.0144
6. Meyers M A, and Murr L E, *Acta Metall* **26** (1978) 951.
7. Gertsman V Y, Tangri K, and Valiev RZ, *Acta Metall Mater* **42**(1994) 785.
8. Moallemi M, Kermanpur A, Najafizadeh A, Rezace A, Baghbadorani H S, and Nezhadfar P D, *Mater Sci Eng A* **653** (2016) **147**.
9. Bruce G, Ph. D. Thesis. A general mechanism of martensitic nucleation (1974) 142.
10. Olson GB, and Cohen M. *Metall Trans A* **7A** (1976) 1897.
11. Cao Y, Wang Y B, Chen Z B, Liao X Z, Kawasaki M, Ringer S P, Langdon T G, and Zhu Y T, *Mater Sci Eng A* **578** (2013) 110.
12. Asgari S, El-Danaf E, Kalidindi S R, and Doherty R D, *Metall Mater Trans A* **28** (1997) 1781.

13. Ueno H, Kakihata K, Kaneko Y, Hashimoto S, and Vinogradov A, *J Mater Sci* **46** (2011) **4276**.
14. Yapici G G, Karaman I, Luo ZP, Maier H J, and Chumlyakov Y I, *J Mater Sci* **19** (2004) 2268.
15. Somekawa H, Watanabe H, Basha D A, Singh A, and Inoue T, *Scripta Mater* **129**(2017) 35.
16. Remy L, *Scripta Mater* **11** (1977) **169**.
17. Lee T H, Oh C S, Kim S J, and Takaki S, *Acta Mater* **55**(2007) 3649.
18. Gutierrez-Urrutia I, Zaefferer S, and Raabe D. *Mater Sci Eng A* **527** (2010) 3552.
19. Rath BB, Imam M A, and Pande C S, *Mater Phys Mech* **1** (2000) 61.
20. Pande C S, Imam M A, and Rath BB, *Metall Trans A* **21** (1990) 2891.
21. Mahajan S, *Acta Mater* **45** (1997) 2633.
22. Lu L, Shen Y, Chen X, Qian L, and Lu K. *Science* **304** (2004) 422.
23. Mathewson C H, *Trans Am Soc Metals* **32** (1944) 38.
24. Murr L E, *Interfacial phenomena in metals and alloys*. Addison-Wesley Pub.Co. advanced book program, (1975) 387.
25. Wang X, Zurob H S, Embury J D, Ren X, and Yakubtsov I, *Mater Sci Eng A* **527**(2010) **3785**.
26. Bouaziz O, Scott C P, and Petitgand G, *Scripta Mater* **60** (2009) 714.
27. Hu H, and Smith C S, *Acta Metall* **4** (1956) 638.
28. Smith C S, and Guttman L, *JOM* **5** (1953) 81.
29. Schramm R E, and Reed R P, *Metall Trans A* **6** (1975) 1345.
30. El-Danaf E, Kalidindi S R, and Doherty R D, *Metall Mater Trans A* **30** (1999) 1223.
31. Blewitt T H, Coltman RR, and Redman JK, *J Appl Phys* **28** (1957) 651.
32. Suzuki H, and Barrett C S, *Acta Metall* **6** (1958) 156.
33. Cottrell A H, Bilby B,A, and Lx A, *Philos Mag Ser* **7** (1951) **573**.
34. Christian J W, and Mahajan S, *Progress Mater Sci* **39** (1995) 1.
35. Mahajan S, and Chin G Y, *Acta Metall* **21** (1973) 353.
36. Fujita H, and Mori T,. *Scripta Metall* **9** (1975) 631.
37. Mori T, and Fujita H, , *Acta Metall* **28** (1980) 771.
38. Niewczas M, and Saada G, *Philos Mag A* **82** (2002) 167. https://doi.org/10.1080/01418610208240003
39. Tewary N K, Ghosh S K, and Chatterjee S *Int J Metall Eng*. **4** (2015) 12. https://doi.org/10.5923/j.ijmee.20150401.03
40. Wang J, Li N, Anderoglu O, Zhang X, Misra A, Huang J Y, and Hirth J P, *Acta Mater* **58** (2010) 2262
41. Fullman RL, and Fisher J C, *J Appl Phys* **22** (1951) 1350.
42. Torrents A, Yang H, and Mohamed F A, *Metall Mater Trans A* 41 (2010) 621–630.
43. Yang B, and Vehoff H, *Mate Sci Eng A* **400**(2005) 467.
44. Westbrook J H, Aust K T, Hanneman R E, and Niessensn P, *Acta Metall* **16** (1968) 291.
45. Wang S J, Jozaghi T, Karaman I, Arroyave R, and Chumlyakov YI, *Mater Sci Eng A*. **694** (2017)121.
46. Bouaziz O, and Barbier D, *J Nanosci Nanotechnol* **12** (2012) 8732.